
Natural Lighting Systems Based on Dielectric Prismatic Film

Daniel Vázquez-Moliní, Antonio Álvarez Fernández-Balbuena
and Berta García-Fernández

Additional information is available at the end of the chapter

<http://dx.doi.org/10.5772/50352>

1. Introduction

Daylight provides high quality lighting, reduces energy use and has numerous beneficial physical and psychological effects on people. Furthermore, natural lighting has many benefits in creating indoor spaces, such as energy saving and better quality of vision; two facts that improve environments and thus, productivity.

The light pipe is a device that can transfer natural light from a building's roof into the depths of the building, this straight construction consist of a reflective closed walled structure (P.D. Swift & G.B. Smith, 1995). Daylight guidance has been one of the mayor areas of innovation in interior lighting in recent years, with the development of light pipes daylight and electric light are simultaneously delivered into a building where they are combined and distributed via luminaries. As a result, the overall wattage of artificial light is reduced and the consumption of electricity decreases (Mayhoub, et al., 2010). The commonest light pipes are reflective mirror guides which use high reflectance aluminium, also fiber optic guides are widely used for illumination purposes. Optical design with new materials like dielectric ones, with regard to their reflection, transmission and absorption is as important as its geometry study.

In recent works, Vazquez-Moliní et al. introduced an illumination system called ADASY® integrated into a building's façade that consists of a horizontal light guide inside the building. ADASY® comprises a collection system, a light guide, and daylight luminaries (Vazquez-Moliní et al, 2009). Prior developments in solar lighting systems based on micro-replicated light film had been studied showing that prism light guides performance varies with the length of the guide, maintenance conditions, the collecting system, the luminaries, and the direction from which light is directed (Whitehead, L. A., 1982). The objective of previous investigations of the group had been the study and development of

efficient dielectric prismatic hollow light pipes that direct natural light into interior spaces applied in office buildings. One of the proposed systems is a daylight illumination system by vertical transparent prismatic light guide for an office building; this model consists in a hollow tube internally coated with thin polycarbonate prismatic film. In this model, two different prismatic sheets have been used; the light guiding system works with 90° prismatic film and the extraction system is composed of 70° prismatic film perpendicular to the previous one that works extracting the light outside the guide with a specific angular distribution. This design allows us to obtain a transparent simple and beautiful pipe which is integrated in building design; in addition, the spatial distribution of the extraction sheets can be adapted to the requirements of each space. (Alvarez Fernandez-Balbuena A. et al, 2010).

Light color quality is an important issue to evaluate in natural lighting systems. High reflectance aluminum lighting guides are giving bad light quality because the spectral reflectance of the aluminium, changes the color characteristics of the output light at the end of the guide (Vázquez-Moliní et al, 2007). When light guides are made of a dielectric prismatic film, the influence of the spectral reflectance is minimized due to the total internal reflection produced in the surface of the prismatic film, absorptance is not usually considered significant in the literature when the sheets are thin. Color Rendering Index and Correlated Color Temperature are important parameters in order to evaluate lighting quality in Museums, office buildings and production centers to get the normative approval (García-Fernández et al, 2011).

A skylight is a technology for obtaining natural light into a building. Skylights are an opening in a roof that is covered with translucent or transparent material and that is designed to admit light provided a connection to the outdoor environment to occupants. Nowadays the skylight technology is widely used in outstanding buildings (Dubois, 2003). Almost all of the skylights used are just an opening in the ceiling that ensures watertight but without significant optics, just a diffuser on it to prevent direct sunlight.

The Compound Parabolic Concentrators (CPC) is a non-focusing light funnel with specular reflecting surface of a parabolic shape designed to give the maximum concentration ratio for a given acceptance angle θ_{max} . CPCs are relevant for solar energy capture because they achieve good concentration for many acceptance angles. There are many applications where the Compound Parabolic Concentrator is used not only for concentration but also for collimation (in reverse mode) like in natural lighting, thermal collector, LED's optic, car light and optical fiber coupling (Winston, 1975). Winston et al. had explored a growing field that is applicable to areas where the collection, concentration, transport and distribution of light is important. Systems for natural light capture offer very important advantages when use some kind of CPC optics (Winston et al., 2005). CPC passive optics made of dielectric film allows the operation of the collimating system during long periods of time without need to fit its orientation since a CPC in reverse mode is capable of redirecting all the light entering in 2π in the designed angle (Alvarez Fernandez-Balbuena et al., 2009).

2. Prismatic film

A prismatic film is a thin plastic that works with the optical principle of total internal reflection (TIR) through the prism structure. It can be used in several applications for replacing metal guides with best performance. The film geometry has one flat surface and the other one is a textured surface consisting of an array of linear right angle prisms inclined at 45 degrees to the flat surface. This configuration has a light angular acceptance cone determined by the refractive index of the prismatic film material, approximately a 30° semiangle cone. If this angular criterion is not met, the light will instead be rejected out of the light pipe through the prismatic material (OLF).

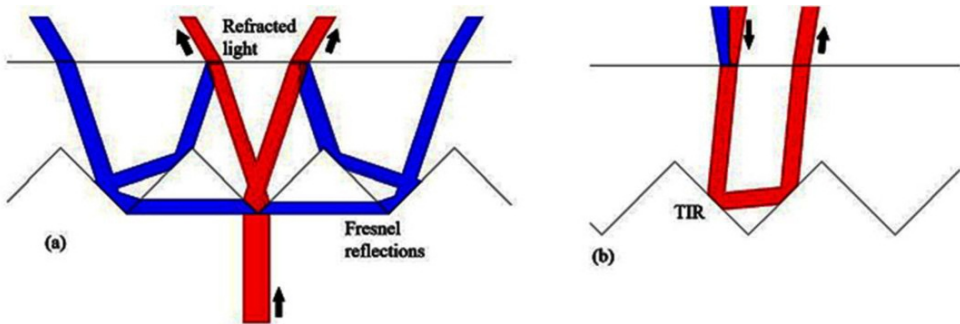


Figure 1. (a) Example of refraction and (b) total internal reflection in prismatic film.

Figure 1 (a) is an example of light entering in a prismatic film through prism apex side, in this case light is divided in two main arms (refracted light). The incident rays are drawn in red lines and the Fresnel refractions are plotted with blue lines. Most of the rays directly emerge from the prism as displayed in red lines; rest of light that is guided in the prismatic structure is Fresnel light with low flux energy. In figure 1 (b) the prismatic film produces TIR, in this case the light is returned in the direction from which it came, this principle is used for guiding light with a prismatic film.

The degree to which the film's prisms deviate from perfect prisms also affects the efficiency of the total internal reflection process, and therefore, the effectiveness of the film in transporting and distributing light. These imperfections include 90° corners which are not precise, surfaces which are not optically flat or which deviate from the correct angle and optical inhomogeneities in the material (Remillard et al.1992). Absorption is due to bulk absorptivity of the material used to produce the film and transmission can be used to advantage of the application in light distribution. With the typical losses due to absorption and transmission, the reflectance efficiency has been estimated as approaching 99% (Keipp, 1994). Precision micromachining, polymer processing and certain other manufacturing technologies like microreplication have made possible the development of an optimized prismatic film (Wang, 2009). The structure of prism film under different magnifications is shown in Figure 2.

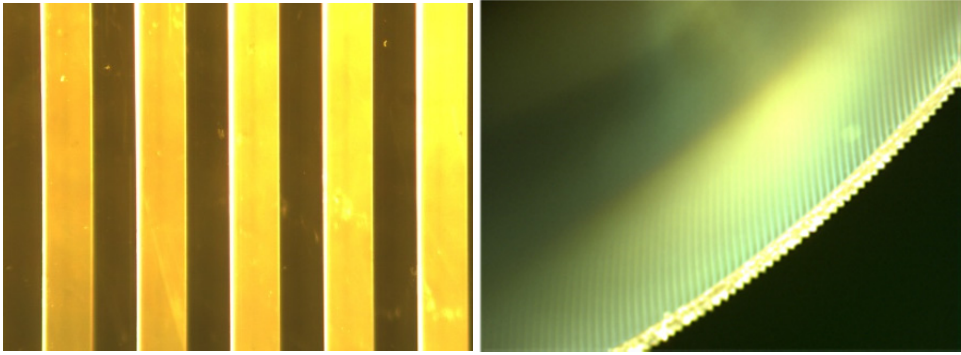


Figure 2. Prismatic film used to distribute light. a) Surface area detail of prisms structure (25X), b) prismatic film (2.5X).

2.1. Image processing algorithms

This section deal with a brief description of the recognition procedure algorithm to analyse the prism profile structure. First, a diagram with a description of the recognition procedure to extract the inclination of the lines from the image and to calculate the radio of the peak prism is given (Fig.3), secondly, a more detailed description will follow.

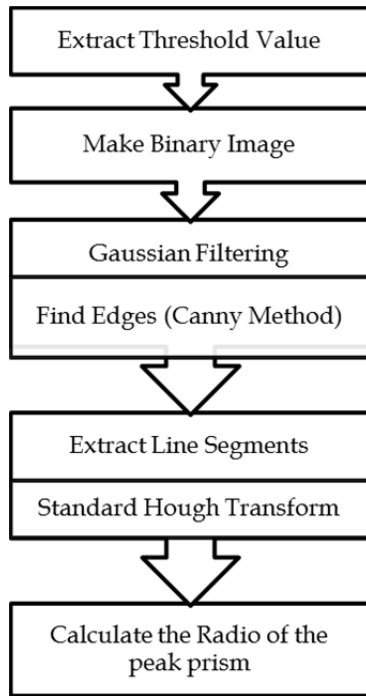


Figure 3. Structure of the recognition procedure and extraction process performed.

In order to investigate the light behavior in the system the effect of accuracy of prismatic structures and peak defects has been examined; computer analyses such as changes of prism angle and plane shape were carried out. By analyzing the image processing prism structure and by using morphological operations measurement of the inclination angle with high accuracy can be achieved. To execute the processing, the prismatic film profile showed in figure 4 is employed (the optical microscope used to obtain the prism image is Motic SMZ-143 equipped with a digital camera Moticom 2000).

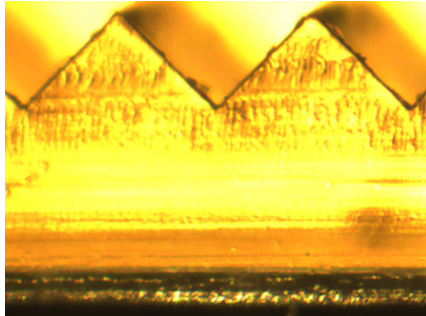


Figure 4. Prism structure used to analyse the parameters of the prism (57X)

Firstly, a threshold is applied to the input image in order to make it binary. The threshold value is determined from a grey-level histogram of the image, later the edge is separated from the background (Fig.5.b).

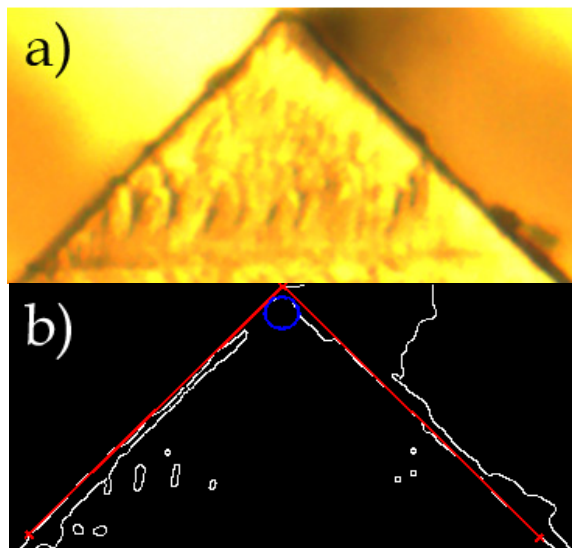


Figure 5. (a) Cropped image before the digital processing used to obtain the dimensions of micro prism structures. (b) Edge detected images resulting from the Canny Method (white), the line after Hough transforms (red), and the estimation to calculate the radius of the prism's peak (blue).

The edge map is used to determine the existence of lines around the regions. This edge description is obtained from the operator Canny (Canny, 1986) this operator is consider as an optimal edge detector to find boundaries between poorly defined objects as well as hard edges. The Canny method finds edges by looking for local maxima of the gradient of the image; the gradient is calculated using the derivative of a Gaussian filter. The method uses two thresholds, to detect strong and weak edges, and includes the weak edges in the output only if they are connected to strong edges.

Later, we use the Hough transform (Fig.5. (b) and Fig.6) to detect the parameters that controls the accuracy of the right angle at the vertex of the prism (Hough, 1962).

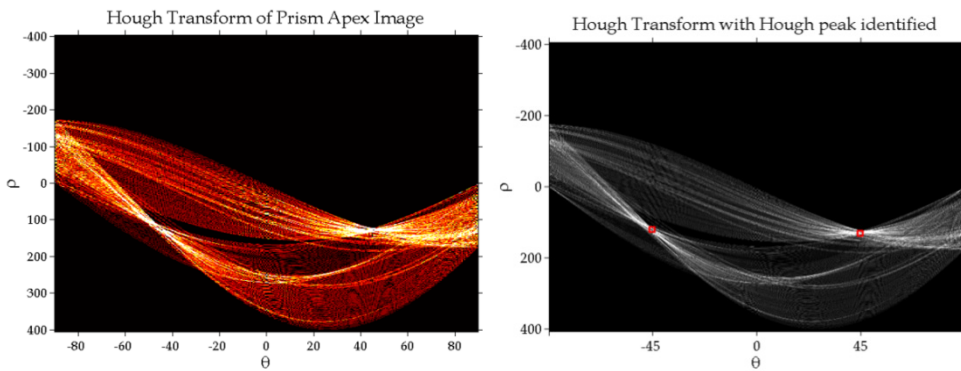


Figure 6. (a) The Hough transform of the prism image. (b)The red square shows the peaks of data in the Hough matrix. ρ is the distance from the center and θ the angle at which the sum of intensities in the image peaks, it is thus the slope of the line along with the position.

Originally, the Hough Transform was proposed to extract straight lines in the particle tracks recognizing procedure. Nowadays, the Hough transform is a technique which is used to insulate features of a particular shape within an image. In this case, the Hough transform is used to identify the parameters of the line and it uses the parametric representation of a line which is fits to a set of given edge points. It takes as input the grey scale image, and produces as output an image showing the positions of tracked intensity discontinuities. The output of the edge detector defines where features are in the image, and the Hough transform determine what the features are and how many of them exist in the image. The main advantage of the Hough transform technique is that it is tolerant of gaps in feature boundary descriptions and is minimal unaffected by image noise. The result of the Hough transform is stored in a matrix that often is considered an accumulator (Fig. 6 (a)). One dimension of this matrix is the angles θ and the other dimension are the distances ρ , and each element has a value telling how many points/pixels are positioned on the line with parameters (ρ, θ) . So the element with the highest value shows the line that is most represented in the input image.

After performing probabilistic Hough Transform, two lines are obtained determining and ensuring the right angle prism used to guide the incident light. Figure 5 shows in blue color the plot of the inclination angle of the prism through the digital processing. The main peaks are located in the Hough transform matrix. The left slope is calculated to be an apex angle of -45.38° and the right slope has an apex angle of 44.50° forming a total angle of 89.88° (Fig. 6 (b)), after that, an approximation was made to relate the prism rounding radius with the slope values and the contour of the vertex profile. The circle obtained used to achieve the radius of the prism vertex is showed in red color (Fig. 5 (b)). The prism base obtained has a width of $400\ \mu\text{m}$ and the radius value obtained is $13.78\ \mu\text{m}$; this result could be affected by the pressure exerted to make the cut of the prism film.

3. Prismatic lightguide analysis

The lightguide structure analysed is a prismatic hollow tube with the thin polycarbonate film with right angle prism sections. The prism light guide transmits light by total internal reflection, which gives higher efficiency and homogeneous light distribution through the guide. Prismatic sheeting developments have provided further improvements in sunlight systems (Fig. 7), boosting efficiency for specific incidence angles with regard to the aluminum guides.



Figure 7. Prismatic light tubes are used for transporting and distributing natural light. Experimental setup in the School of Optics (Complutense University of Madrid)

Light travels mainly in the hollow air space inside the guide and bounces off by total internal reflections (TIR) when the input light is highly collimated. This configuration has an angular acceptance cone, which is not an isotropic distribution in the space determined by the refractive index of the prismatic film, if the refractive index of the dielectric material is

1.5, as is the case of acrylic plastic, then the input light angle must be approximately less than 27.5° from the guide's axial direction, even though the acceptance cone can be higher in the meridional plane.

Two different analysis have been done: Firstly, a theoretical simulation based on the specular reflection model in order to analyse the color characteristics to the output of two guides, rectangular and cylindrical of different lengths, one of them of aluminum material and the other one, internally coated of prismatic film structure this model have been developed by means of a mathematical software as Matlab. Secondly, the prismatic guides proposal evaluates with a ray tracing software through which we show the efficiency for a wavelength evaluated at the end of the guide, this model have been studied with Monte Carlo ray tracing.

3.1. Theoretical simulation

The analysis presented is based on the specular reflection model. There are two important objectives to evaluate with regard to the light quality as a function of the Spectral Power Distribution; these are Correlated Color Temperature (CCT) and the Color Rendering Index (CRI) of the light source, which we evaluate in this work using the guidelines of CIE 13.3.

Color rendering of an illuminant is the effect of the illuminant on the color appearance of objects by conscious or subconscious comparison with their color appearance under a reference illuminant. Colour Rendering serves to describe the effect of an illuminant on the color appearance of objects. The most fundamental natural source is daylight, thus the primary reference for comparing the rendering of a source should be the Standard Illuminant D65.

The Correlated Color Temperature is the temperature of the Planckian radiator whose perceived color most closely resembles that of a given stimulus at the same brightness and under specified viewing conditions (CIE 17.4, 1989). According to this definition, CCT can be calculated using one of the chromaticity diagrams. CIE still recommends to calculate CCT using the 1960 (u, v) chromaticity diagram (now deprecated). On the (u, v) diagram, find the point on the Planckian locus that is at the shortest distance from the given chromaticity point. CCT is the temperature of the Planck's radiation at that point. CCT can be calculated from CIE 1931 chromaticity coordinates x and y in many different ways. Complicated algorithms and simple equations alike have been proposed and used for several decades.

The simulated construction of the prismatic guides is based on a tube internally coated polycarbonate sheet whose outer face is composed of 90° micro-prisms; rays that enter on the guide with an angle suitable undergo total internal reflections. In this model, in order to include the round in corners and the absorption we estimate the spectral reflectance of the inner face of the prism sheet will be estimated in 0.99 throughout the spectrum analyzed. In this section two different types of light guides: circular and rectangular cross sections have been analyzed (Fig. 8).

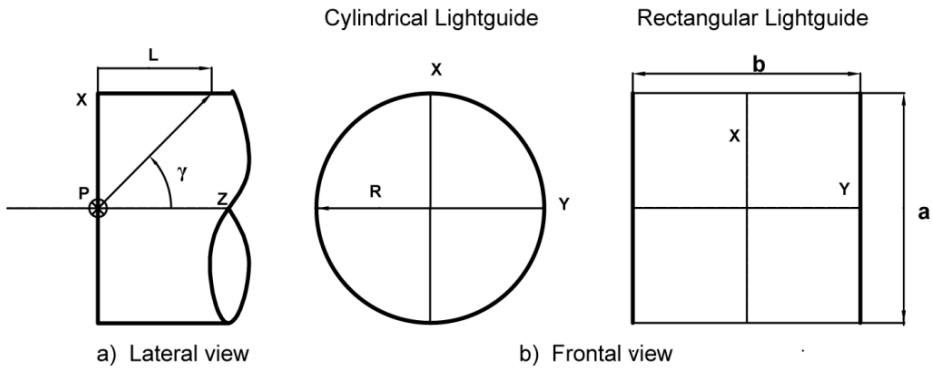


Figure 8. The Coordinate system defines the angles of incidence and observation in the guides. Longitudinal section (a) and transverse section (b).

The photometric profile of the source is an angular distribution adapted to the optimal transmission features of the prismatic film used, and the analysis was restricted to the spectral range between 380 and 780 nm. The CIE Illuminant D65 is the reference light source.

The spectral reflectance of aluminum is estimated as isotropic over the fence and has been experimentally determined using a Hitachi U-3400 spectrophotometer with special accessories for measuring the specular reflectance at 12° incidence. Experimental spectral reflectance measured of aluminum is shown in figure 9.

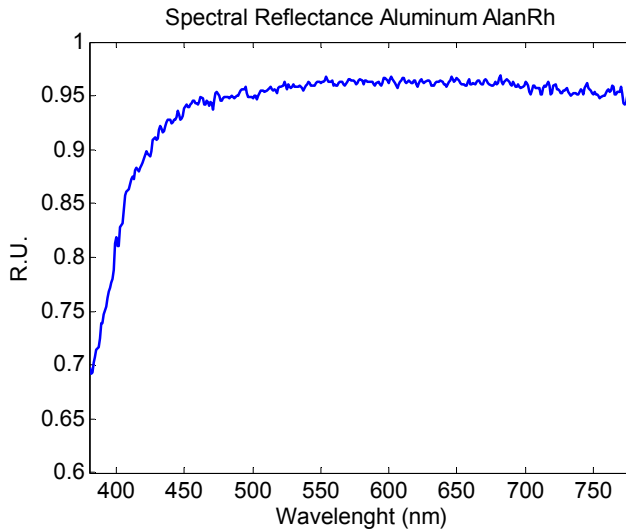


Figure 9. Aluminum spectral reflectance.

To determine the spectral distribution of radiation emerging from the rectangular guide, it is used the model developed by Whitehead (Whitehead, L.A., 1982). According to this model, the number of traversals (Δn) per unit length (Δz) of a ray of light undergoes inside the guide is given by the following expression:

$$\frac{\Delta n}{\Delta z} = \frac{\tan \theta}{Dr}, \quad (1)$$

where Dr is the average cross-sectional distance travelled by a ray in crossing the guide air space and θ is the angle by which any ray deviates from the guide's axial direction.

If the guide air space is rectangular, with dimensions a and b (fig.8), then

$$Dr = (a^{-1} + b^{-1})^{-1}, \quad (2)$$

If roughly circular with radius R

$$Dc = \frac{4R}{\pi}, \quad (3)$$

In the rectangular case, the dimension a is the same as b (0.8862 meters), the cylindrical guide aperture radius is 0.5 meters in order to maintain the same input area than rectangular guide, and the length of the guides (L) evaluated are 5, 10 and 15 meters.

The dependence of the radiant flux with the angle to the incident beam is given by equation 4

$$\varphi(\theta) = 2\pi I_0 [\cos \theta_2 - \cos \theta_1], \quad (4)$$

where I_0 is the total intensity power radiated by the source in a specific direction θ . Moreover, we obtain the spectral distribution of radiant flux incident S_λ , where S_λ is the primary illuminant spectral distribution. θ_1 and θ_2 are the angular limits and the intensity has I_0 value.

The spectral and angular distribution at the exit of the guide will be:

$$S' = \int_0^{\pi/2} P(\lambda, \theta) \rho(\lambda, \theta)^n d(\lambda, \theta), \quad (5)$$

ρ is the reflectance of the material for each wavelength studied and n is considering the number of internal reflections obtained for each incidence angle θ in the guide.

The prismatic guide has a higher transmission throughout the spectrum (Fig. 10) and the relative spectral power is constant. In the aluminum guide, the energy area of the shorter wavelengths obtained is reduced due to low spectral reflectance of the aluminum.

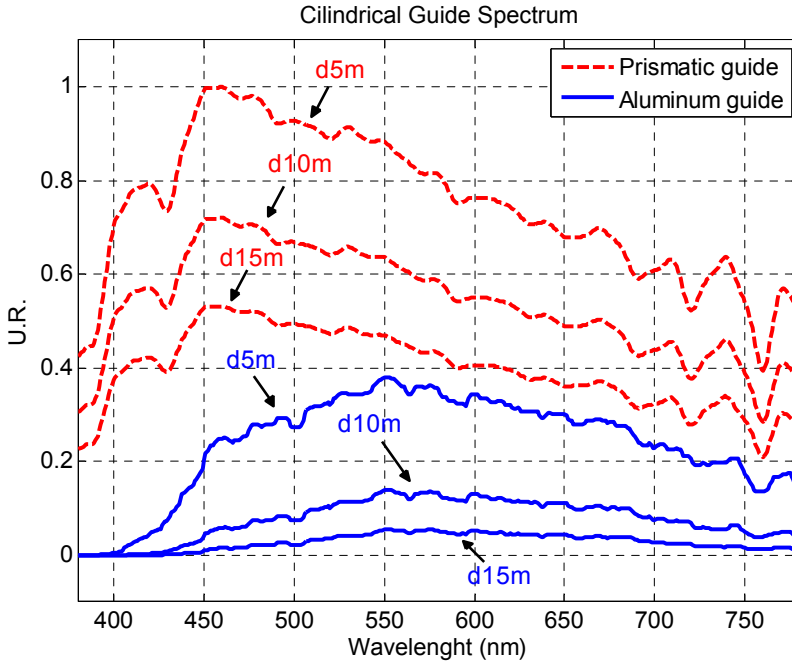


Figure 10. Spectral Power Distribution of the two types of guides for different lengths.

3.2. Color analysis for circular and rectangular lightguides

The spectral power distribution is used for the estimation of the spectral ratio resulting. The spectral ratio is used to compare the spectral distribution at the input and output of the guides. The spectral ratio (η_λ) will be:

$$\eta(\lambda) = \frac{S'(\lambda)}{S(\lambda)} \tag{6}$$

Considering $S(\lambda)$ the input spectral power distribution of the source and $S'(\lambda)$. Spectral power distribution ratio emergence from cylindrical guide is greater from rectangular guides with the same dimensions (figure 11). In addition, the ratio decreases significantly in 10 and 15 meters from aluminum guides. The prismatic guide has high transmission across the spectrum and the spectral power is constant. There is a downward trend in short wavelengths in aluminum guide energy due to the spectral reflectance characteristics of the material.

We define the spectral ratio, η_λ as the fraction of the incident spectral power distribution transmitted by the guide:

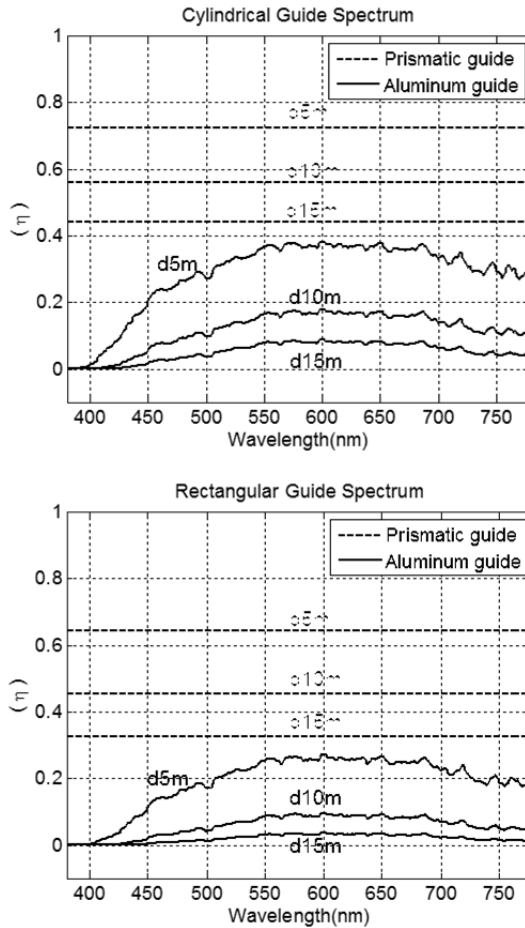


Figure 11. The ratio of spectral power distribution of the two types of guides for different lengths.

For comparing different behavior of light guide regarding color output flux it is used CIE 1931 diagram due to it is more spread on known color representation (CIE 13:3, 1995).

Color coordinates in CIE 1931 chromaticity diagram for studied lengths of aluminum and prismatic guides are show in figure 12. The chromatic coordinates with the light source (D65) chosen for different lengths of guide will be compared. The three consecutive black square points and blue circle points represent the aluminum guide in 5, 10 and 15 meters.

The three consecutive points (d5m, d10m and d15m) represent the aluminum guide. The results of the CIE 1931 chromaticity coordinates of the full spectrum transmitted in the prismatic guides differ from those transmitted in the aluminum guides approaching to the yellow zone. When the length of the aluminum guides increases, there are no changes in the results obtained for the prismatic guide (P), and the result are superposed with the illuminant D65 because the reflectance is maintained for the entire spectrum.

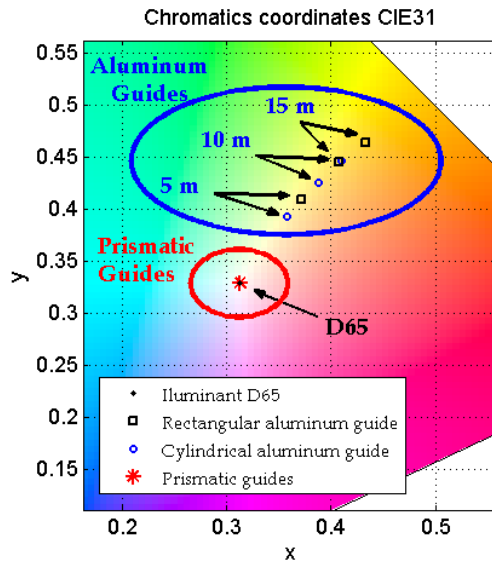


Figure 12. CIE 1931 chromatic coordinates of the studied lightguides.

The CCT is obtained from the spectral distribution at the exit of the guide (Table 1). This calculation is carried out for different lengths of the two types of guides considered in this work. To determine the reference light source for a given test source, we must find the CCT of the test source. Once this data is known, the reference light source is a Planckian black body which has the same temperature.

Moreover, the Color Rendering Index (CRI) of the sources at the end of the guides it is calculated (fig.13). From the result obtained (Fig.10), it is possible to determine the significant color change in the aluminum fence, showing less color change difference for all lengths than the prismatic guides.

	Cylindrical Guide		Rectangular Guide	
	CCT (°K)	CRI	CCT (°K)	CRI
Illuminant D65	6503	99.97	6503	99.97
Prismatic guide (5m)	6503	99.97	6503	99.97
Prismatic guide (10m)	6503	99.97	6503	99.97
Prismatic guide (15m)	6503	99.97	6503	99.97
Aluminum guide (5m)	4707	89.81	4407	87.74
Aluminum guide (10m)	4126	85.45	3818	82.39
Aluminum guide (15m)	3781	81.98	3478	78.15

Table 1. Correlated Color Temperature (CCT) and Color Rendering Index of each spectral power.

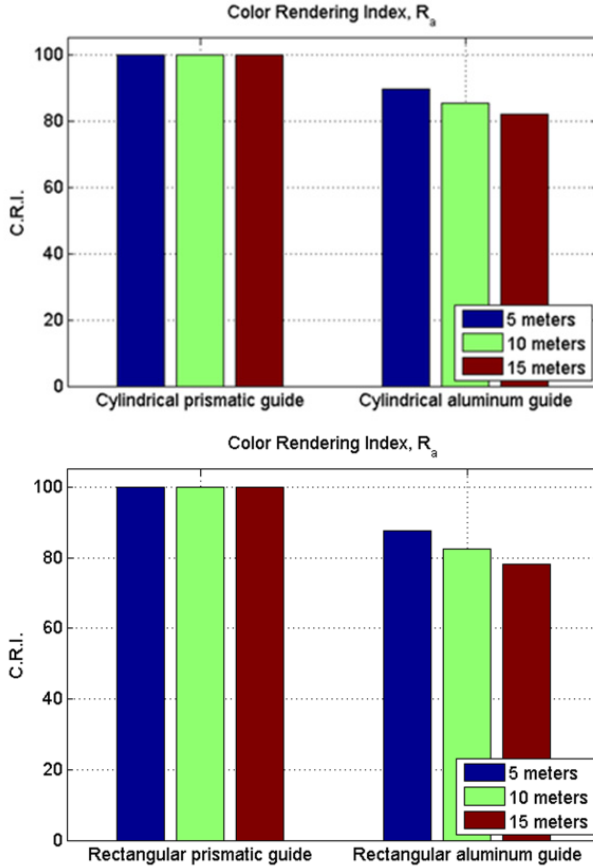


Figure 13. CRI of measured lightguides (cylindrical and rectangular).

3.3. Flux transfer analysis

The flux transmitted of the two types of prismatic guides for a wavelength is studied in order to analyze the efficiency of both systems. For this purpose, the distribution characteristics are calculated using a three-dimensional ray tracing. In this case, the lightguides have a 1.49 refractive index for the studied wavelength without absorption losses. Generally, the associated absorption loss in prismatic film is rather low, and taking into account that it is considered the model of light reflection, in this study this parameter will not be studied on the color quantity estimated.

The dimensions of the guides analyzed in the ray tracing study (Fig.14) are the same defined in the theoretical simulation (Fig.8) and the enlargement scale factor of the prism shape is on the order of 10. The light cone input is an extensive emitter with a random distribution of 30° semi angle (θ) which has the same size as the section of the light guide.

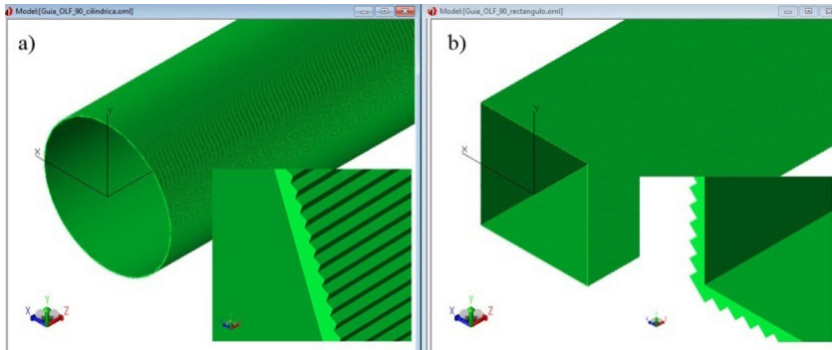


Figure 14. Perspective view of Ray trace simulation model of lightguides with a detail of the prismatic structure: cylindrical (a) and rectangular (b).

The comparison of efficiency in rectangular and cylindrical prismatic guides is shown in Figure 15; the graphics indicates the influence of the shape in maintaining the transported flux and the efficiency for a wavelength (546 nm). The output flux efficiency of 15 meters cylindrical guide is 2% higher than rectangular guide; in addition, in the first meters the flux remains more constant.

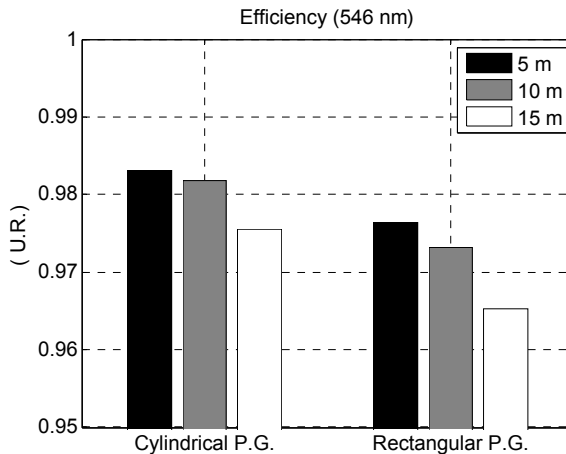


Figure 15. Output efficiency results for wavelength of 546 nm in Prismatic Guides.

4. Hollow prismatic CPC

Compound parabolic concentrator (CPC) is an optical devices used in the solar energy related areas and also in other applications where radiant energy concentration is needed, being defined as one of the first devices that resulted from the practical application of nonimaging optics (Welford and Winston, 1978). Light from a defined range of angles of incidence is reflected by total internal reflection on the parabolic walls of the CPC and concentrated at the exit of the CPC.

The authors propose an innovative 3D hollow prismatic CPC (PCPC) in reverse mode made of a prismatic dielectric material, which has a high efficiency comparing it with aluminium CPC (ACPC). The basic idea is to use a hollow prismatic light guide with CPC shape. In figure 16 (up-left), we can observe the design in 2D geometry in the inverse mode proposal; all the rays entering at the focus of the parabola (F_1 and F_2) emerge through the exit aperture with the design angle θ . This paper reports 2D, 3D design (Fig. 16) and numerical analysis by ray-tracing software, furthermore experimental results are shown. A prototype has been developed and tested showed in figure 16 (down). The hollow PCPC in reverse mode has an entrance pupil that is small compared to the exit pupil depending on the design angle. This CPC design accepts light in 2π entering the entrance pupil and redirecting it in the CPC design angle. This new concept is made of a prismatic film; this dielectric layer accepts light not only in the entrance pupil (Entry 1) but also through the layer itself. This property allows an increase in efficiency compared with the ACPC.

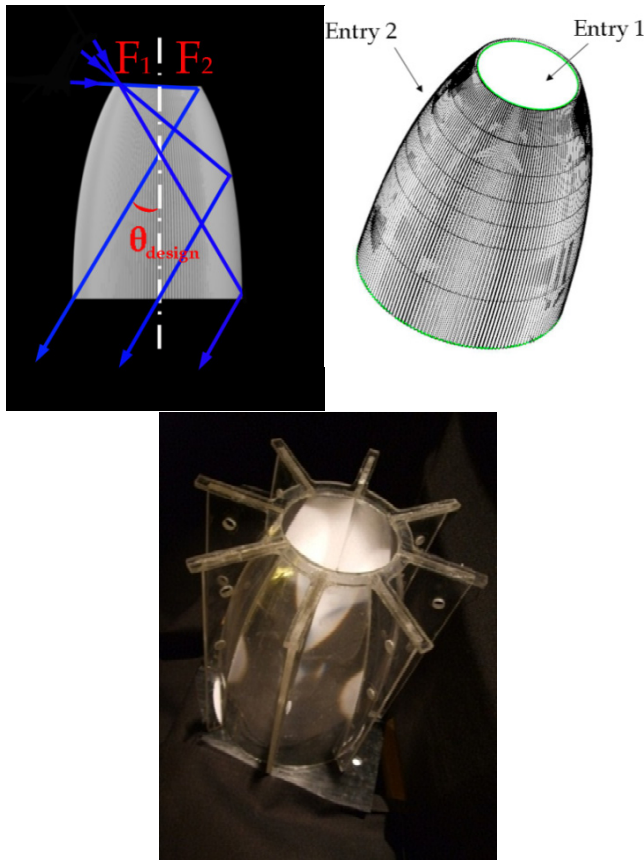


Figure 16. The CPC profile (up-left) with a ray tracing showing the design angle and the maximum input angle of design θ , 3D hollow HCPC 30° software design (up-right) and the experimental prototype (down) in which the reflector surface is a prismatic film supported by eight polycarbonate ribs.

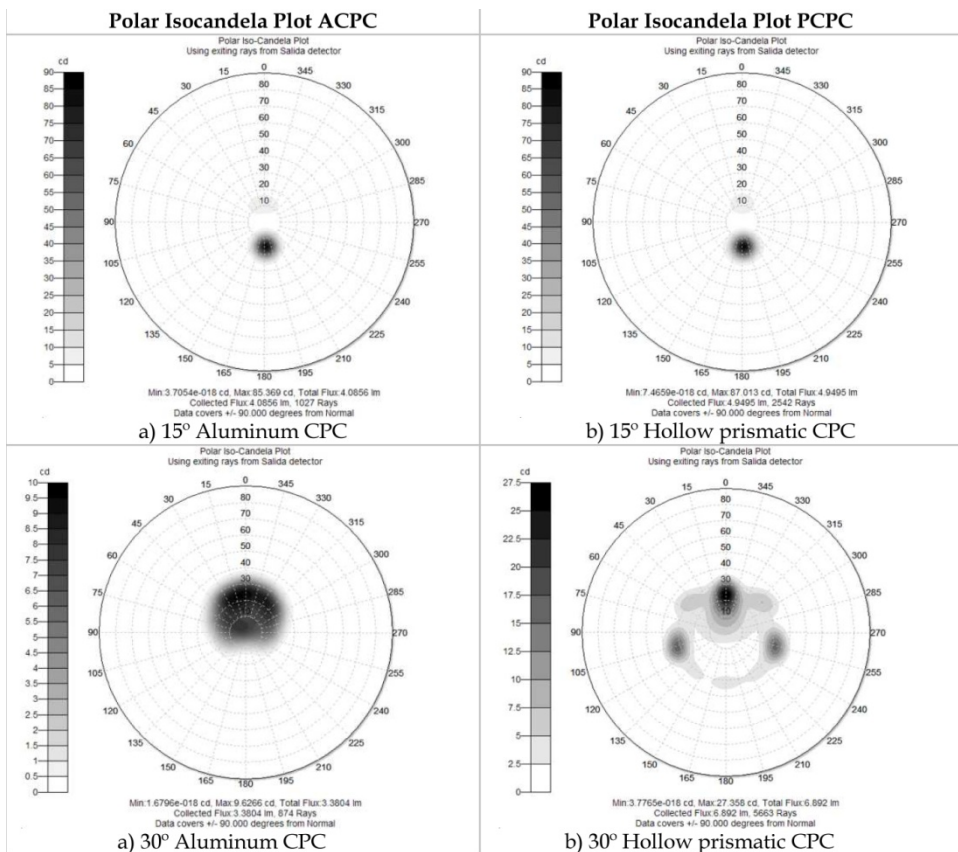
In this section we analyzed the PCPC by raytracing software to determine the angular transmission, optical efficiency and irradiance distribution on the system exit aperture in a 3D system, later a comparison between ACPC and PCPC is presented.

4.1. Ray-tracing: Efficiency of the PCPC compared to ACPC

Ray-tracing is processed for two kinds of CPCs, one designed with standard aluminum with a reflectance of 1.0 and the other one, the prismatic CPC designed with PMMA.

4.1.1. Polar Isocandela Plot of ACPC and hollow PCPC

The polar intensity diagram provides the shape of the light distribution of both parabolic systems. Figure 17 (a) shows isocandela plot representing the ACPC intensity and angular distribution. The 17 (b) illustrations show the isocandela plot for PCPC when light enter through entry 1+2.



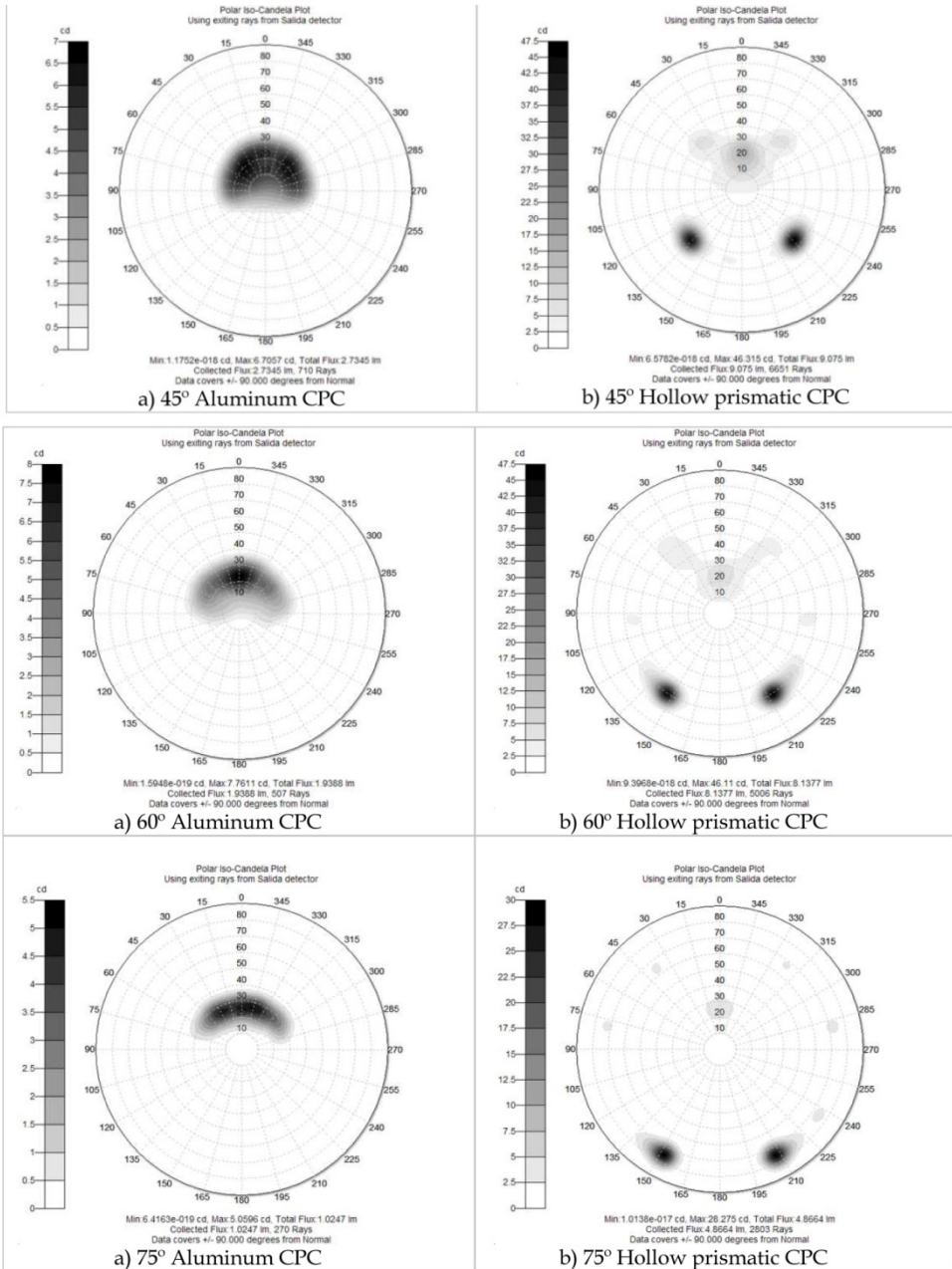


Figure 17. The polar intensity diagram provides the shape of the light distribution to the exit of both parabolic systems

5. Efficiency comparative

Ray-tracing is processed for two kinds of CPCs, one designed with standard aluminum with a reflectance of 100 % and the other one, designed with dielectric prismatic film.

Computed efficiency is obtained by tracing collimated rays in 5° angle intervals for both systems and computing the obtained flux at the exit pupil of the system.

The comparison of PCPC and ACPC collectors is shown in figure 18; it indicates the effects of incidence angles and the efficiency of the PCPC. To compare both systems it is used collimated light at different angles. The flux obtained in the entry 1 (Φ) is used to calculate the final efficiency (η),

$$\eta = \frac{\phi_{\text{entry1}}}{\phi_{\text{exitpupil}}} \quad (7)$$

The PCPC accepts light out of this entry pupil Entry 1 so η can be higher than 100%.

When it is analysed the efficiency obtained in both systems adding the prismatic surface of the PCPC (entry1+entry2) to 85°, it is observed the improvement with regard to the ACPC, reaching a 600 % higher efficiency flux than an ACPC.

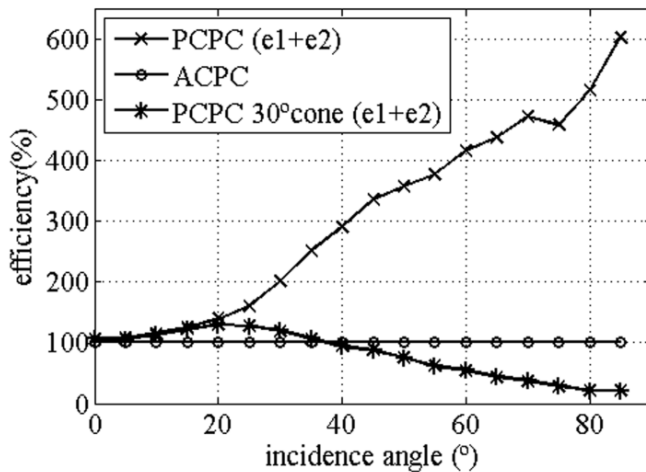


Figure 18. Output flux HPCPC VS output flux HPCPC 30° cone using entry1 and entry2

The efficiency of the PCPC to compare the outflow of 30° cone (*) (entry1+entry2) with regard to the efficiency of entry 1 it is evaluated. There is a clear profit for incidence angles ranging from 0° to 35°, though it is necessary to improve the efficiency for the higher incidence angles.

It is necessary to investigate how the PCPC is working when light enters in the entry pupil (entry 1) as it is done in ACPC.

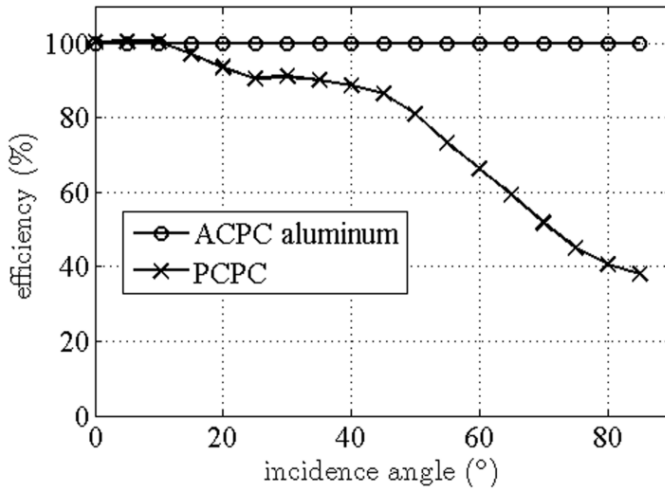


Figure 19. ACPC VS PCPC using entry 1.

The ACPC works better than PCPC as the incidence angle increases if we use only entry 1 in the prismatic PCPC. Figure 19 shows this behaviour for different incidence angles. The TIR that suffers light beam in the outer surface of the PCPC is not happening when incidence angle increases, this behavior explains the decrease of efficiency according to the incidence angle increases. The division of the beam showed in figure 20 (b) is due to the prismatic effect when light reach the film in the outer side as shown basic raytrace in figure 1a.

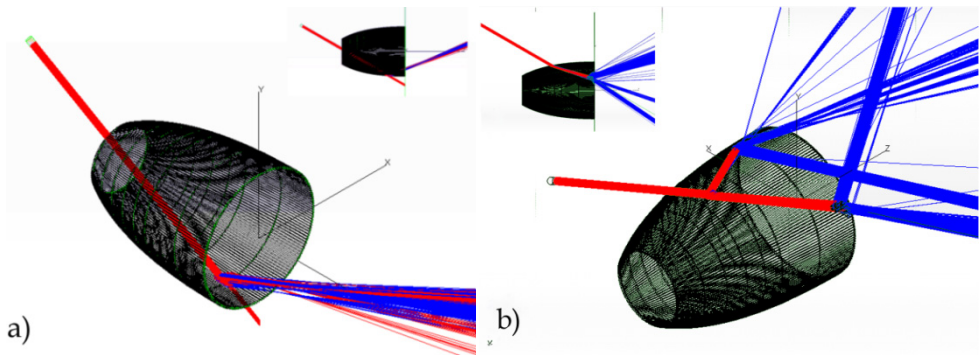


Figure 20. Examples of collimated light entering entry 1 30° (a) and entry 2 30° (b).

The light guiding after PCPC is a good alternative to light far away from the collecting system, the use of a hollow light guide is demonstrated as a good way to transport light, and new bending systems show a good way to reach all the lighting necessities.

6. Experimental measures

A CCD video photometer (Radiant Imaging Prometric 1400) is used to measure output light distribution in exit pupil with a Lambertian screen (Fig.21). We measure output light in two experimental assemblies changing the incidence angle between 0° and 75° increasing the source angle in steps of 15° . Firstly, we evaluate entry 1, and secondly entry 1+2 is evaluated.

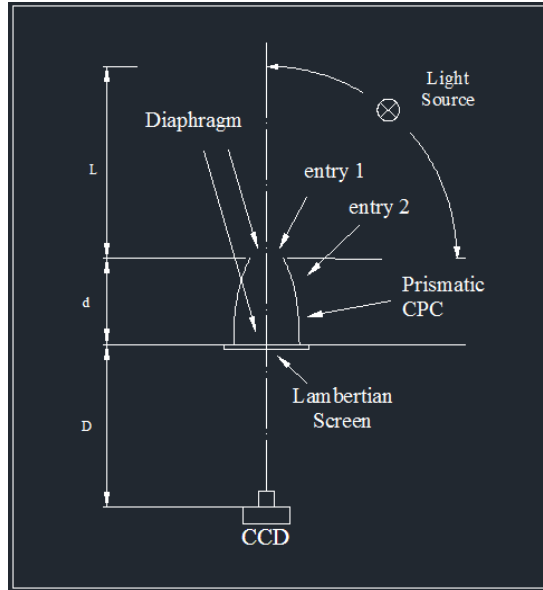


Figure 21. Schematic diagram of experimental setup The HPCPC has the following parameters: input aperture diameter (entry1): 88 mm; output aperture diameter (Lambertian screen): 187 mm, L: 4000 mm, d: 260 mm.

Normalized light distribution map onto exit pupil is shown in the figures 22 to 28. The (a) figure represents the illuminance map obtained with the ray tracing software, the (b) figure represents the map obtained with the experimental setup. Figures 22 to 24 show data for using entry 1 and 25 to 28 show data using entry 1+entry 2 for some light angles.

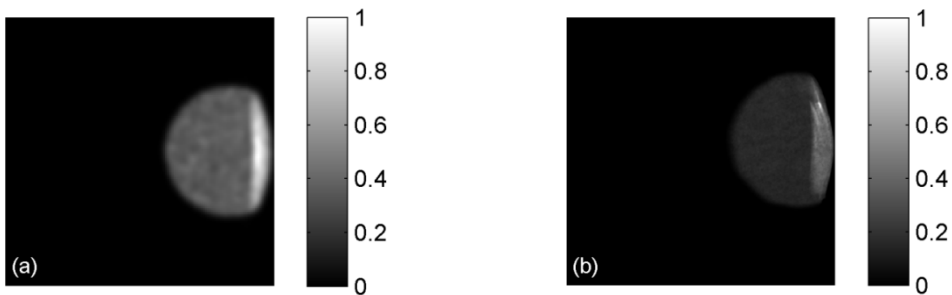


Figure 22. 15° entry1. (a) Raytracing simulation, (b) Experimental measurement.

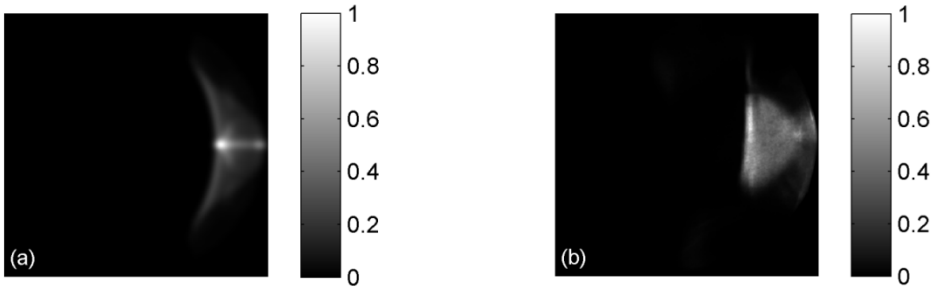


Figure 23. 30° entry1. (a) Raytracing simulation, (b) Experimental measurement.

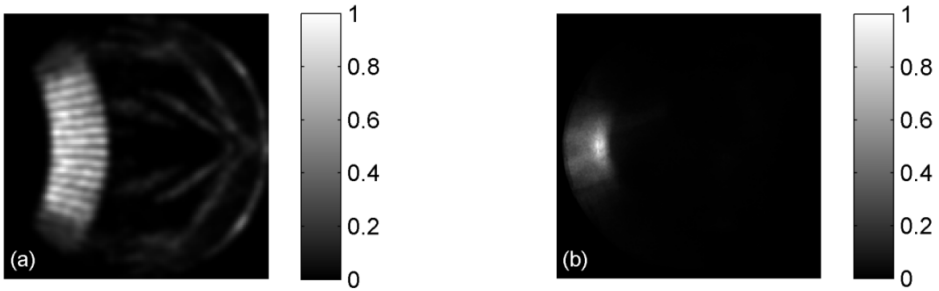


Figure 24. 75° entry1. (a) Raytracing simulation, (b) Experimental measurement.

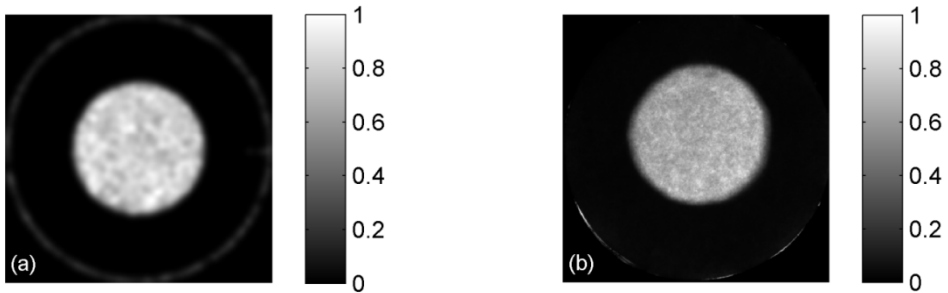


Figure 25. 0° entry1+entry2. (a) Raytracing simulation, (b) Experimental measurement.

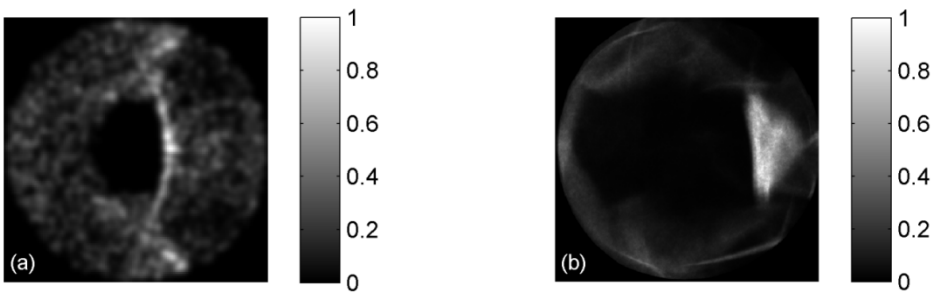


Figure 26. 45° entry1+entry2. (a) Raytracing simulation, (b) Experimental measurement.

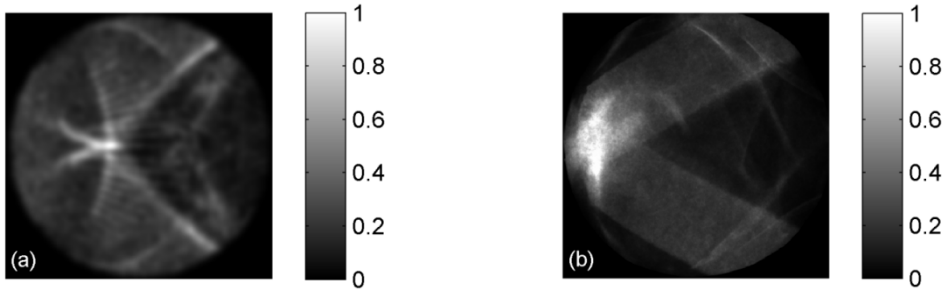


Figure 27. 60° entry1+entry2. (a) Raytracing simulation, (b) Experimental measurement.

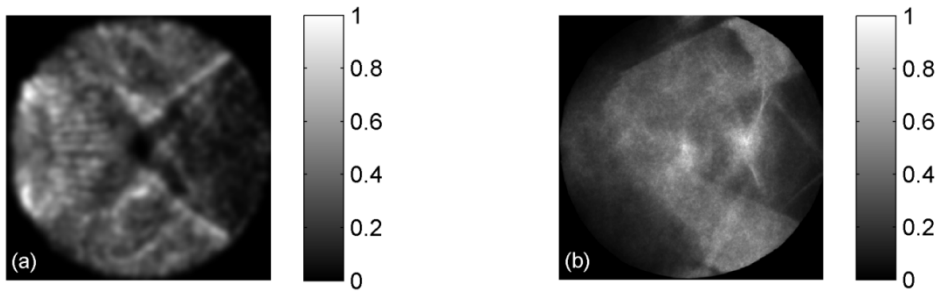


Figure 28. 75° entry1+entry2. (a) Raytracing simulation, (b) Experimental measurement.

The circular peripheral wreath in figure 25 is due to the multiple internal reflections of the light inside the prismatic film. When we increase the angle of incidence, we can observe the division of the beam showed in figure 27 due to the prismatic film structure.

7. Conclusions

The present study shows the interesting combination of light transmission and reflection capabilities of dielectric prismatic film analysed in different guidance geometries and the approach of a collecting system for sunlight applications. Prismatic film can work as a perfect mirror or transparent material depending upon the angle that light strikes the material, it allow us to produce lighting products with unique properties.

It is important to analyse the micro-structure prism imperfections in the form of the surfaces: imperfect corners (apex and valley), surfaces which are not optically flat or which deviate from the expected angle, optical inhomogeneities in the material and the existence of the curved area on the peaks prism which modify the optical behaviour of the prism film; this imperfections modify the optical path and therefore the rays can be directed to other directions instead of undergoing total internal reflections. In order to check the importance of prism rounding, the apex is analysed through Hough Transform by digital image processing. The peak curved radio obtained is despised because of the radius size obtained

by image processing is small with regard to the size of the prism structure. The prism are calculated to have an angle of 89.88° and the diameter of the curved region obtained in the prism's peak is $27.56 \mu\text{m}$, this result could be affected by the pressure exerted to make the cut of the film.

Dielectric prismatic guides have a high quality output flux regarding standard light guides based on specular material. Specific shapes such as a circular cross section show a soft increase in flux transmission, with the extent of the improvement dependent on the input position of the light ray.

When input light is in the admitted angle the prismatic light guides have a higher transmission in the entire spectrum than the reflective guides and their spectral efficiency is more constant. There is a downward trend in short wavelength in aluminum guide energy due to the spectral reflectance characteristics of the material.

Prismatic light guides turn out to be more robust in lighting quality maintenance than the aluminum guides, which are efficient but only capable of maintaining light quality distances lower than 5 meters. Cylindrical light guides have a 2% higher efficiency than rectangular although the rectangular shape could be more convenient in office buildings due to the occupied space and construction constraints.

In this study, the authors propose an innovative 3D hollow prismatic CPC (PCPC) working in reverse mode and made of a dielectric material, which has a high efficiency compared with aluminium CPC (ACPC). Transportation of daylight over longer distances requires an optimized collector, the PCPC is an appropriate design for natural light systems like skylights and collector guiding systems since it has properties as collimator to catch the light and to direct it and transport it long distances from a remote source with little attenuation. The hollow PCPC has an entrance pupil that is small compared to the exit pupil depending on the design angle. This CPC design accepts light in 2π entering the entrance pupil and redirecting it in the CPC design angle. This new concept is made of a prismatic structure film; this dielectric layer accepts light not only in the entrance pupil but also through the layer itself.

The results obtained shows that measured PCPC efficiency compared with standard aluminum is 600% higher at 85° incidence angle, a medium value of 300% increase is obtained in the range from 0 to 85° . There is a clear profit for incidence angles ranging from 0° to 35° , though it is necessary to improve the efficiency for the higher incidence angles.

The design of big structures in buildings is easier with this new system because of the minor weight of the plastic material which can be conformed in independent parts and development in moulding fabrication can improve the cost of the system.

Author details

Daniel Vázquez-Moliní, Antonio Álvarez Fernández-Balbuena and Berta García-Fernández
Dept. of Optics, School of Optics, University Complutense of Madrid, Spain

8. References

- Alvarez Fernandez-Balbuena A., Vázquez-Moliní D., Garcia-Fernandez B., Garcia-Botella A. & Bernabeu E. (2009). Skylight: a hollow prismatic CPC, *Proceedings of the SPIE*, 7423, 74230T.
- Alvarez Fernandez-Balbuena A., Vázquez-Moliní D., García-Fernandez B., García-Rodríguez L. & Galán-Cañestro T. (2010) Daylight illumination system by vertical Transparent Prismatic Lightguide for an office building. *Colour and Light in Architecture*. Knemesi, Verona, pp. 360-365.
- Canny, J. (1986). A Computational Approach to Edge Detection, *IEEE Trans. Pattern Analysis and Machine Intelligence*, 8(6):679–698.
- CIE Publ. No.13.3 (1995). Technical Report- *Method of measuring and specifying colour rendering properties of light source*.
- CIE Publ. No.17.4 (1989). IEC Pub. 50(845) *International.Lighting Vocabulary*.
- Dubois, M.D. (2003). Shading devices and daylight quality: an evaluation based on simple performance indicators, *Lighting Research and Technology*, 35(1): 61-74
- García-Fernández, B., Vázquez-Moliní, D. & Álvarez Fernández-Balbuena, A. (2011). Lighting quality for aluminum and prismatic light guides. *Proceedings of the SPIE* 8170, 81700T.
- García-Botella A, A. Fernández-Balbuena A., Vázquez-Moliní D. & Bernabéu E. (2009), Ideal 3D asymmetric concentrator, *Solar Energy*, 83 pp. 113-119. Hough, P.V.C. (1962). Methods and means for recognizing complex patterns, U.S. Patent 3,069,654, Dec.
- Hsieh, C. K. (1981). Thermal analysis of CPC collectors *Solar Energy*, 27 (1): 19-29.
- Remillard J.T., Everson M.P. & Weber W.H. (1992). Loss mechanisms in optical light pipes, *Applied Optics*, 31(34):7232-7241.
- Kneipp, K.G. (1994). Use of prismatic films to control light distribution, *International Lighting in Controlled Environments Workshop*, NASA-CP-95-3309, pp. 307-318.
- Mayhoub M. S. & Carter D J. (2010). Towards hybrid lighting systems: A review, *Lighting Research and Technology*, 42:51-71.
- Wang M.W. & Tseng C.C. (2009). Analysis and fabrication of a prism film with roll-to-roll fabrication process. *Optics Express*, 17(6):4718-4725.
- OLF 2301 Data sheet, www.3M.com/lightingproducts.
- Swift P.D. & Smith G.B. (1995). Cylindrical mirror light pipes, *Solar Energy Materials and Solar Cells*, 36(2) 159-168.
- TracePro® Opto-Mechanical Design Software, <http://www.lambdare.com/>
- Vázquez-Moliní D., Álvarez Fernández-Balbuena A., González-Montes M., Bernabeu E., García-Botella A., García-Rodríguez L., and Pohl W. (2009), Guiding daylight into a building for energy-saving illumination. SPIE Newsroom, *Proceedings of the SPIE* DOI: 10.1117/2.1200911.1825.
- Welford, W.T. & Winston, R (1978). *The Optics of Nonimaging Concentrators: Light and Solar Energy*. Academic Press, London.

- Winston, R. (1975). Development of the compound parabolic collector for photo-thermal and photo-voltaic applications *Proceedings of the Society of Photo-Optical Instrumentation Engineers*. Optics in Solar Energy Utilization, 68: 136-44.
- Winston, R., Miñano, J. C. & Benitez P. (2005). *Nonimaging Optics*, Elsevier Academic Press, San Diego, CA.
- Whitehead, L. A. (1981). U. S. Patent 4,260,220. *Prism Light Guide Having Surfaces which are in Octature*.
- Whitehead, L. A. (1982). Simplified Ray Tracing in Cylindrical Systems, *Applied Optics*, 21(19): 3536-3538.